G^3-SPLINES FOR THE PATH PLANNING OF WHEELED MOBILE ROBOTS

Aurelio Piazzi, Massimo Romano, and Corrado Guarino Lo Bianco

Università di Parma - Dipartimento di Ingegneria dell'Informazione,
Parco Area delle Scienze, 181/A - I-43100 Parma - Italy,
Tel. + 39 0521 905733, Fax. + 39 0521 905723,
E-mail: {piazzi, romano, guarino }@ce.unipr.it

Keywords: path planning, wheeled mobile robots, dynamic path inversion, polynomial splines, iterative steering.

Abstract

This paper deals with generation of smooth paths for the navigation of wheeled mobile robots by means of the iterative steering technique. A new motion planning primitive called G^3-spline or η-spline is proposed. It is a seventh order polynomial spline that permits the interpolation of an arbitrary sequence of points with associated arbitrary direction, curvature and curvature derivative. Adopting this path planning, the robot's control inputs can be obtained by means of a dynamic path inversion procedure ensuring the continuity of velocities and accelerations. This new spline depends on a vector with six parameters (η) that can be used to finely shape the path. The paper includes both theoretical results and path planning examples.

1 Introduction

The advisability of pursuing a path planning with continuous curvatures for wheeled mobile robots (WMRs) was early indicated by Nelson [8] who devised two primitives, quintic curves for lane changing maneuvers and polar splines for symmetric turns, to smoothly connect line segments. Subsequently, many authors have worked on various planning schemes ensuring continuous-curvature paths, for example [2], [3], [12], [4]. In particular the authors have proposed in [9], [10] a continuous-curvature path planning based on a new parameterized curve, called G^2-spline. This motion primitive was adopted to achieve a straightforward inversion-based control for the iterative steering of vision-based autonomous vehicles.

In this paper we propose a generalization of the quintic G^2-spline leading to the G^3-spline, also called η-spline. It is a seventh order polynomial spline that permits the interpolation of an arbitrary sequence of points with associated arbitrary direction (unit tangent vector), curvature and curvature derivative. In such a way, not only the path curvature is continuous but also the derivative with respect of the arc length of the curvature is overall continuous too. Adopting this path planning, as showed in [6], the robot's control inputs can be obtained by means of a dynamic path inversion procedure ensuring the continuity of velocities and accelerations. In particular, the overall continuity of the robot's linear and angular accelerations is achieved by planning with the G^3-splines whereas using the G^2-splines leads to the sole continuity of the robot's velocities (in this case accelerations can be discontinuous). Hence a definite benefit is gained with the G^3-splines. Moreover, this new spline depends on a vector with six parameters (η) that can be used to finely shape the robot's path.

The paper is organized as follows. Section 2 introduces the new concept of G^3-paths or paths with third order geometric continuity and the related inversion based control of WMRs. Section 3 is the core of the paper: the G^3-splines are presented with their explicit closed-form parameterizations and related completeness and minimality results are included (Proposition 2 and Property 1). A result on the symmetry of the proposed η-parameterization is exposed in Section 4 with path planning examples. Concluding remarks are given in Section 5

2 G^3-Paths and inversion based smooth control of WMRs

A curve on the $\{x,y\}$-plane can be described by means of the map $\mathbf{p}:[u_0,u_1]\to\mathbb{R}^2$, $u\to p(u)=[\alpha(u)\,\beta(u)]^T$, where $[u_0,u_1]$ is a real closed interval. The associated "path" is the image of $[u_0,u_1]$ under the vectorial function $\mathbf{p}(u)$, i.e. $\mathbf{p}([u_0,u_1])$. We say that the curve $\mathbf{p}(u)$ is regular if $\dot{\mathbf{p}}(u)\in C_p([u_0,u_1])$ and $\dot{\mathbf{p}}(u)\neq 0\ \forall u\in[u_0,u_1]$ (here and in the following the class of piecewise continuous functions is denoted by C_p). The curve length measured along $\mathbf{p}(u)$, denoted by s, can be expressed with the function $f:[u_0,u_1]\to[0,f(u)]$, $u\to s=\int_{u_0}^{u}\|\dot{\mathbf{p}}(\xi)\|\,d\xi$, where $\|\cdot\|$ denotes the Euclidean norm. Given a regular curve $\mathbf{p}(u)$, the length function $f(\cdot)$ is continuous over $[u_0,u_1]$ and bijective; hence its inverse is continuous too and will be denoted by $f^{-1}:[0,f(u_1)]\to[u_0,u_1]$, $s\to u=f^{-1}(s)$.
Associated with every point of a regular curve $\mathbf{p}(u)$ there is the orthonormal moving frame $\{\boldsymbol{\tau}(u),\boldsymbol{\nu}(u)\}$ that is congruent with the axes of the $\{x,y\}$-plane and where $\boldsymbol{\tau}(u)=\dot{\mathbf{p}}(u)/\|\dot{\mathbf{p}}(u)\|$ denotes the unit tangent vector of $\mathbf{p}(u)$. For any regular curve such that $\ddot{\mathbf{p}}(u)\in C_p([u_0,u_1])$, the scalar curvature is well defined according to the Frenet formula $\frac{d\boldsymbol{\tau}}{ds}(u)=\kappa_c(u)\boldsymbol{\nu}(u)$ so that we have the function $\kappa_c:[u_0,u_1]\to\mathbb{R}$, $u\to\kappa_c(u)$. The scalar curvature can also be expressed as a function of the curve length s, i.e. $\kappa:[0,f(u_1)]\to\mathbb{R}$, $s\to\kappa(s)$; evidently this function can be evaluated as $\kappa(s)=\kappa_c(f^{-1}(s))$.

Definition 1 *(G^1-,G^2- and G^3-curves) A parametric curve*

$\mathbf{p}(u)$ *has first order geometric continuity and we say* $\mathbf{p}(u)$ *is a* G^1*-curve if* $\mathbf{p}(u)$ *is regular and its unit tangent vector is a continuous function along the curve, i.e.* $\tau(\cdot) \in C^0([u_0,u_1])$. *The curve* $\mathbf{p}(u)$ *has second order geometric continuity and we say* $\mathbf{p}(u)$ *is a* G^2*-curve if* $\mathbf{p}(u)$ *is a* G^1*-curve,* $\ddot{\mathbf{p}}(\cdot) \in C_p([u_0,u_1])$ *and its scalar curvature is continuous along the curve, i.e.* $\kappa_c(\cdot) \in C^0([u_0,u_1])$, *or equivalently,* $\kappa(\cdot) \in C^0([0, f(u_1)])$. *The curve* $\mathbf{p}(u)$ *has third order geometric continuity and we say* $\mathbf{p}(u)$ *is a* G^3*-curve if* $\mathbf{p}(u)$ *is a* G^2*-curve,* $\dddot{\mathbf{p}}(\cdot) \in C_p([u_0,u_1])$ *and the derivative with respect to the arc length s of the scalar curvature is continuous along the curve, i.e.* $\dot{\kappa}(\cdot) \in C^0([0, f(u_1)])$.

G^1- and G^2- curves where introduced by Barsky and Beatty [1] in a computer graphics contest and the G^3-curves has been recently proposed by the authors [6] for the inversion-based control of WMRs. Moreover, a "natural" definition of G^i-paths on the Cartesian plane is the following.

Definition 2 *(G^1-, G^2- and G^3-paths) A path of a Cartesian space, i.e. a set of points of this space, is a G^i-path ($i = 1,2,3$) if there exists a parametric G^i-curve whose image is the given path.*

Consider as a motion model of a wheeled mobile robot the following nonholonomic system:

$$\begin{cases} \dot{x}(t) &= v(t)\cos\theta(t) \\ \dot{y}(t) &= v(t)\sin\theta(t) \\ \dot{\theta}(t) &= \omega(t) \end{cases} \tag{1}$$

where x, y indicate the robot position with respect to a stationary frame, θ is the robot heading angle, and v , ω are its linear and angular velocities to be considered as the control inputs of the robot.
In order to achieve a smooth control of the robot the inputs $v(t)$ and $\omega(t)$ must be C^1-functions, i.e. the linear and angular accelerations of the robot are continuous signals. It is useful to define an "extended state" of model (1) that comprises the inputs and their derivatives:

$$\{x(t), y(t), \theta(t), v(t), \dot{v}(t), \omega(t), \dot{\omega}(t)\}.$$

Then, the following Smooth Motion Planning Problem (SMPP) can be posed [6].
SMPP: Given any assigned travelling time $t_f > 0$, find control inputs $\dot{v}(\cdot)$, $\omega(\cdot) \in C^1([0,t_f])$ such that the mobile robot starting from an arbitrary initial extended state

$$\mathbf{p}_A = [x_A\, y_A]^T = [x(0)\, y(0)]^T,\ \theta_A = \theta(0),$$

$$v_A = v(0),\ \dot{v}_A = \dot{v}(0),\ \omega_A = \omega(0),\ \dot{\omega}_A = \dot{\omega}(0),$$

reaches the arbitrary final extended state

$$\mathbf{p}_B = [x_B\, y_B]^T = [x(t_f)\, y(t_f)]^T,\ \theta_B = \theta(t_f),$$

$$v_B = v(t_f),\ \dot{v}_B = \dot{v}(t_f),\ \omega_B = \omega(t_f),\ \dot{\omega}_B = \dot{\omega}(t_f).$$

The solution of the above problem, exposed in [6], can be used in a motion control architecture based on the iterative steering approach [7]. In such a way, swift high-performance motion of the WMR can be achieved while intelligent or elaborate behaviours are performed. The solution to SMPP is based on a path dynamic inversion procedure that needs a planning of a G^3-path connecting $\mathbf{p}_A$ with $\mathbf{p}_B$. This relies on the following result.

Proposition 1 *[6] A path* Γ *on the Cartesian plane is generated by the model (1) with inputs* $v(\cdot)$, $\omega(\cdot) \in C^1$, $v(t) \neq 0$, $\forall t \geq 0$ *if and only if* Γ *is a* G^3*-path.*

The G^3-path connecting $\mathbf{p}_A$ with $\mathbf{p}_B$ must satisfy interpolating conditions at the end-points that depend on the initial and final extended states of the WMR. Consider, for example, the case $v_A > 0$ and $v_B > 0$. Then the heading angles of the initial and final pose of the WMR are the angles, θ_A and θ_B, with respect to the x- axis of the unit tangent vectors at the path end-points (see Fig. 1). Mooreover, the curvatures and the derivatives with

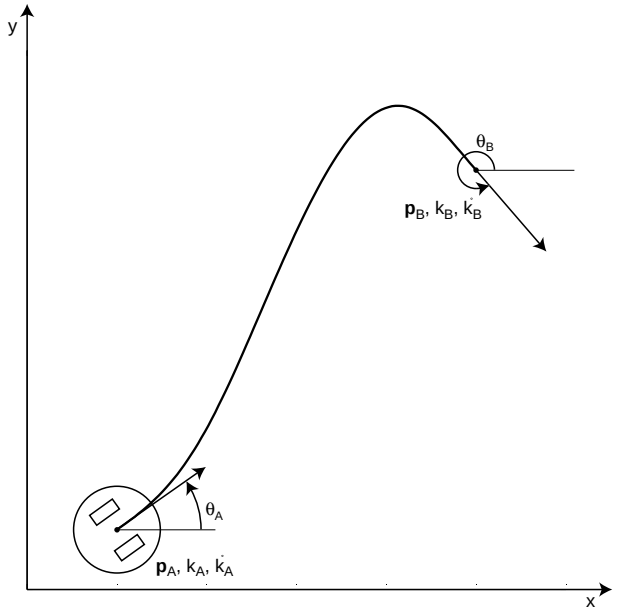

Figure 1: A G^3-path connecting $\mathbf{p}_A$ with $\mathbf{p}_B$ and satisfying end-point interpolating conditions.

respect to the arc length of the curvatures at the end-points can be determined according to the expressions:

$$k_A = \frac{\omega_A}{v_A} \quad , \quad k_B = \frac{\omega_B}{v_B}$$
$$\dot{k}_A = \frac{\dot{\omega}_A v_A - \omega_A \dot{v}_A}{v_A^3} \quad , \quad \dot{k}_B = \frac{\dot{\omega}_B v_B - \omega_B \dot{v}_B}{v_B^3}$$

The critical case $v_A = 0$ and/or $v_B = 0$ and other cases are discussed in [6].

3 Polynomial G^3-splines

In the context of the smooth iterative steering of WMRs, the previous section has shown the necessity of planning with G^3-paths having arbitrary interpolating conditions at the end-points. This justifies the introduction of the following problem.

The polynomial G^3-interpolating problem: *D*etermine the minimal order polynomial curve that interpolates between given points $\mathbf{p}_A = [x_A\, y_A]^T$ and $\mathbf{p}_B = [x_B\, y_B]^T$ with associated unit tangent vectors defined by angles θ_A and θ_B, scalar curvatures κ_A and κ_B and the derivatives with respect to the arc length of the curvature $\dot{\kappa}_A$ and $\dot{\kappa}_b$ (see Fig. 1). All the interpolating data $\mathbf{p}_A, \mathbf{p}_B \in \mathbb{R}^2$, $\theta_A, \theta_B \in [0, 2\pi)$, $\kappa_A, \kappa_B \in \mathbb{R}$ and $\dot{\kappa}_A, \dot{\kappa}_B \in \mathbb{R}$ can be arbitrarily assigned.

To solve the posed interpolating problem, consider a seventh order polynomial curve $\mathbf{p}(u) = [\alpha(u)\ \beta(u)]^T$, $u \in [0,1]$ where

$$\alpha(u) := \alpha_0 + \alpha_1 u + \alpha_2 u^2 + \alpha_3 u^3 + \alpha_4 u^4 + \alpha_5 u^5 + \alpha_6 u^6 + \alpha_7 u^7 \tag{2}$$

$$\beta(u) := \beta_0 + \beta_1 u + \beta_2 u^2 + \beta_3 u^3 + \beta_4 u^4 + \beta_5 u^5 + \beta_6 u^6 + \beta_7 u^7 \tag{3}$$

The interpolating conditions are the following:

$$\mathbf{p}(0) = \mathbf{p}_A, \qquad \mathbf{p}(1) = \mathbf{p}_B \tag{4}$$

$$\boldsymbol{\tau}(0) = \begin{bmatrix} \cos\theta_A \\ \sin\theta_A \end{bmatrix}, \qquad \boldsymbol{\tau}(1) = \begin{bmatrix} \cos\theta_B \\ \sin\theta_B \end{bmatrix} \tag{5}$$

$$\kappa_c(0) = \kappa_A, \qquad \kappa_c(1) = \kappa_B \tag{6}$$

$$\dot{\kappa}_c(0) = \dot{\kappa}_A \|\dot{\mathbf{p}}(0)\|, \qquad \dot{\kappa}_c(1) = \dot{\kappa}_B \|\dot{\mathbf{p}}(1)\| \tag{7}$$

$\boldsymbol{\tau}(u)$ is the unit tangent vector and is given by $\dot{\mathbf{p}}(u)/\|\dot{\mathbf{p}}(u)\|$. The polynomial curve of the seventh order satisfying all the above conditions has the following coefficients:

$$\alpha_0 = x_A \tag{8}$$

$$\alpha_1 = \eta_1 \cos\theta_A \tag{9}$$

$$\alpha_2 = \frac{1}{2}\eta_3 \cos\theta_A - \frac{1}{2}\eta_1^2 \kappa_A \sin\theta_A \tag{10}$$

$$\alpha_3 = \frac{1}{6}\eta_5 \cos\theta_A - \frac{1}{6}\left(\eta_1^3 \dot{\kappa}_A + 3\eta_1\eta_3\kappa_A\right)\sin\theta_A \tag{11}$$

$$\begin{aligned}\alpha_4 &= 35(x_B - x_A) - \left(20\eta_1 + 5\eta_3 + \frac{2}{3}\eta_5\right)\cos\theta_A \\ &\quad + \left(5\eta_1^2\kappa_A + \frac{2}{3}\eta_1^3\dot{\kappa}_A + 2\eta_1\eta_3\kappa_A\right)\sin\theta_A \\ &\quad - \left(15\eta_2 - \frac{5}{2}\eta_4 + \frac{1}{6}\eta_6\right)\cos\theta_B \\ &\quad - \left(\frac{5}{2}\eta_2^2\kappa_B - \frac{1}{6}\eta_2^3\dot{\kappa}_B - \frac{1}{2}\eta_2\eta_4\kappa_B\right)\sin\theta_B\end{aligned} \tag{12}$$

$$\begin{aligned}\alpha_5 &= -84(x_B - x_A) + (45\eta_1 + 10\eta_3 + \eta_5)\cos\theta_A \\ &\quad - \left(10\eta_1^2\kappa_A + \eta_1^3\dot{\kappa}_A + 3\eta_1\eta_3\kappa_A\right)\sin\theta_A \\ &\quad + \left(39\eta_2 - 7\eta_4 + \frac{1}{2}\eta_6\right)\cos\theta_B \\ &\quad + \left(7\eta_2^2\kappa_B - \frac{1}{2}\eta_2^3\dot{\kappa}_B - \frac{3}{2}\eta_2\eta_4\kappa_B\right)\sin\theta_B\end{aligned} \tag{13}$$

$$\begin{aligned}\alpha_6 &= 70(x_B - x_A) - \left(36\eta_1 + \frac{15}{2}\eta_3 + \frac{2}{3}\eta_5\right)\cos\theta_A \\ &\quad + \left(\frac{15}{2}\eta_1^2\kappa_A + \frac{2}{3}\eta_1^3\dot{\kappa}_A + 2\eta_1\eta_3\kappa_A\right)\sin\theta_A \\ &\quad - \left(34\eta_2 - \frac{13}{2}\eta_4 + \frac{1}{2}\eta_6\right)\cos\theta_B \\ &\quad - \left(\frac{13}{2}\eta_2^2\kappa_B - \frac{1}{2}\eta_2^3\dot{\kappa}_B - \frac{3}{2}\eta_2\eta_4\kappa_B\right)\sin\theta_B\end{aligned} \tag{14}$$

$$\begin{aligned}\alpha_7 &= -20(x_B - x_A) + \left(10\eta_1 + 2\eta_3 + \frac{1}{6}\eta_5\right)\cos\theta_A \\ &\quad - \left(2\eta_1^2\kappa_A + \frac{1}{6}\eta_1^3\dot{\kappa}_A + \frac{1}{2}\eta_1\eta_3\kappa_A\right)\sin\theta_A \\ &\quad + \left(10\eta_2 - 2\eta_4 + \frac{1}{6}\eta_6\right)\cos\theta_B \\ &\quad + \left(2\eta_2^2\kappa_B - \frac{1}{6}\eta_2^3\dot{\kappa}_B - \frac{1}{2}\eta_2\eta_4\kappa_B\right)\sin\theta_B\end{aligned} \tag{15}$$

$$\beta_0 = y_A \tag{16}$$

$$\beta_1 = \eta_1 \sin\theta_A \tag{17}$$

$$\beta_2 = \frac{1}{2}\eta_3 \sin\theta_A + \frac{1}{2}\eta_1^2\kappa_A \cos\theta_A \tag{18}$$

$$\beta_3 = \frac{1}{6}\eta_5 \sin\theta_A + \frac{1}{6}\left(\eta_1^3\dot{\kappa}_A + 3\eta_1\eta_3\kappa_A\right)\cos\theta_A \tag{19}$$

$$\begin{aligned}\beta_4 &= 35(y_B - y_A) - \left(20\eta_1 + 5\eta_3 + \frac{2}{3}\eta_5\right)\sin\theta_A \\ &\quad - \left(5\eta_1^2\kappa_A + \frac{2}{3}\eta_1^3\dot{\kappa}_A + 2\eta_1\eta_3\kappa_A\right)\cos\theta_A \\ &\quad - \left(15\eta_2 - \frac{5}{2}\eta_5 + \frac{1}{6}\eta_6\right)\sin\theta_B \\ &\quad + \left(\frac{5}{2}\eta_2^2\kappa_B - \frac{1}{6}\eta_2^3\dot{\kappa}_B - \frac{1}{2}\eta_2\eta_4\kappa_B\right)\cos\theta_B\end{aligned} \tag{20}$$

$$\begin{aligned}\beta_5 &= -84(y_B - y_A) + (45\eta_1 + 10\eta_3 + \eta_5)\sin\theta_A \\ &\quad + \left(10\eta_1^2\kappa_A + \eta_1^3\dot{\kappa}_A + 3\eta_1\eta_3\kappa_A\right)\cos\theta_A \\ &\quad + \left(39\eta_2 - 7\eta_4 + \frac{1}{2}\eta_6\right)\sin\theta_B \\ &\quad - \left(7\eta_2^2\kappa_B - \frac{1}{2}\eta_2^3\dot{\kappa}_B - \frac{3}{2}\eta_2\eta_4\kappa_B\right)\cos\theta_B\end{aligned} \tag{21}$$

$$\begin{aligned}\beta_6 &= 70(y_B - y_A) - \left(36\eta_1 + \frac{15}{2}\eta_3 + \frac{2}{3}\eta_5\right)\sin\theta_A \\ &\quad - \left(\frac{15}{2}\eta_1^2\kappa_A + \frac{2}{3}\eta_1^3\dot{\kappa}_A + 2\eta_1\eta_3\kappa_A\right)\cos\theta_A \\ &\quad - \left(34\eta_2 - \frac{13}{2}\eta_4 + \frac{1}{2}\eta_6\right)\sin\theta_B \\ &\quad + \left(\frac{13}{2}\eta_2^2\kappa_B - \frac{1}{2}\eta_2^3\dot{\kappa}_B - \frac{3}{2}\eta_2\eta_4\kappa_B\right)\cos\theta_B\end{aligned} \tag{22}$$

$$
\begin{aligned}
\beta_7 \;=\;& -20\,(y_B-y_A)+\left(10\eta_1+2\eta_3+\frac{1}{6}\eta_4\right)\sin\theta_A\\
&+\left(2\eta_1^2\kappa_A+\frac{1}{6}\eta_1^3\dot{\kappa}_A+\frac{1}{2}\eta_1\eta_3\kappa_A\right)\cos\theta_A\\
&+\left(10\eta_2-2\eta_4+\frac{1}{6}\eta_6\right)\sin\theta_B\\
&-\left(2\eta_2^2\kappa_B-\frac{1}{6}\eta_2^3\dot{\kappa}_B-\frac{1}{2}\eta_2\eta_4\kappa_B\right)\cos\theta_B \qquad (23)
\end{aligned}
$$

The real parameters η_i, $i=1,\ldots,6$, appearing in expressions (8)-(23) can be packed together to form the six-dimentional parameter vector $\boldsymbol{\eta}=[\eta_1 \quad \eta_2 \quad \eta_3 \quad \eta_4 \quad \eta_5 \quad \eta_6]^T$, so that the resulting parametric curve can be concisely denoted as $\mathbf{p}(u;\boldsymbol{\eta})$ or, informally, *$\boldsymbol{\eta}$-spline*.
Moreover denote with $\mathcal{H}$ the set given by the Cartesian product $(\mathbb{R}^+)^2\times\mathbb{R}^4$. The main result of this section is given by the following proposition.

Proposition 2 *Given any interpolating data $\mathbf{p}_A$, θ_A, κ_A, $\dot{\kappa}_A$ and $\mathbf{p}_B$, θ_B, κ_B, $\dot{\kappa}_B$, the parametric curve $\mathbf{p}(u;\boldsymbol{\eta})$ satisfies conditions (4)-(7) for all $\boldsymbol{\eta}\in\mathcal{H}$. Conversely, any seventh order polynomial curve $\mathbf{p}(u)$ with $\dot{\mathbf{p}}(0)\neq 0$, $\dot{\mathbf{p}}(1)\neq 0$ satisfying conditions (4)-(7) there exists a parameter vector $\boldsymbol{\eta}\in\mathcal{H}$ such that the curve $\mathbf{p}(u)$ can be expressed as $\mathbf{p}(u;\boldsymbol{\eta})$.*

Proof. For brevity the proof is omitted. It can be found in [11].

Proposition 2 makes evident that the $\boldsymbol{\eta}$-spline is a complete parameterization of all the seventh order polynomial curves interpolating the given endpoint data.

Property 1 *The curve $\mathbf{p}(u;\boldsymbol{\eta})$ is the minimal order polynomial curve interpolating any arbitrarily given data $\mathbf{p}_A$, $\mathbf{p}_B\in\mathbb{R}^2$, θ_A, $\theta_B\in[0,2\pi)$, κ_A, $\kappa_B\in\mathbb{R}$ and $\dot{\kappa}_A$, $\dot{\kappa}_B\in\mathbb{R}$.*

Proof. The seventh degree curve $\mathbf{p}(u;\boldsymbol{\eta})$ characterize all the polynomial curves, interpolating the given endpoint data, till to the seventh order. Hence, if a lower order polynomial curve exists this must coincide with $\mathbf{p}(u;\boldsymbol{\eta})$ for some appropriate $\boldsymbol{\eta}\in\mathcal{H}$. Consider the following interpolating data (leading to a lane-change path):

$$
\mathbf{p}_A=[0\;0]^T,\quad \mathbf{p}_B=[2\;1]^T,
$$
$$
\theta_A=\theta_B=0,\quad \kappa_A=\kappa_B=0,\quad \dot{\kappa}_A=\dot{\kappa}_B=0
$$

$$
\begin{aligned}
\alpha(u;\boldsymbol{\eta}) &= \eta_1 u+\frac{1}{2}\eta_3 u^2+\frac{1}{6}\eta_5 u^3\\
&+\left[70-20\eta_1+5\eta_3+\frac{2}{3}\eta_5-15\eta_2+\frac{5}{2}\eta_4-\frac{1}{6}\eta_6\right]u^4\\
&+\left[168+45\eta_1+10\eta_3+\eta_5+39\eta_2-7\eta_4+\frac{1}{2}\eta_6\right]u^5\\
&+\left[140-36\eta_1-\frac{15}{2}\eta_3-\frac{2}{3}\eta_5-34\eta_2+\frac{13}{2}\eta_4-\frac{1}{2}\eta_6\right]u^6\\
&+\left[-40+10\eta_1+2\eta_3+\frac{1}{6}\eta_5+10\eta_2-2\eta_4+\frac{1}{6}\eta_6\right]u^7\\
\beta(u;\boldsymbol{\eta}) &= 35u^4-84u^5+70u^6-20u^7
\end{aligned}
$$

Evidently it is not possible to interpolate the given data with a sixth or lower order polynomial curve for any arbitrary choice of $\boldsymbol{\eta}\in\mathcal{H}$. □

The following result shows how the $\boldsymbol{\eta}$-splines become line segments under particular interpolating conditions (for a proof see [11]).

Property 2 *(line segments generation) Define $d=\|\mathbf{p}_B-\mathbf{p}_A\|$ and assume $x_B=x_A+d\cos\theta$, $y_B=y_A+d\sin\theta$, $\theta_A=\theta_B=\theta\in[0,2\pi)$, $\kappa_A=\kappa_B=0$, $\dot{\kappa}_A=\dot{\kappa}_B=0$. Then the path generated by $\mathbf{p}(u;\boldsymbol{\eta})$ is a segment line $\forall\boldsymbol{\eta}\in\mathcal{H}$.*

4 Path planning with the G^3-splines

The practical use of the devised G^3-splines requires, apart imposing the interpolating end-points condition, the setting of the η_i parameters ($i=1,2,...,6$). From the relations $\|\dot{\mathbf{p}}(0;\boldsymbol{\eta})\|=\eta_1$ and $\|\dot{\mathbf{p}}(1;\boldsymbol{\eta})\|=\eta_2$ the parameters η_1 and η_2 can be interpreted as "velocity" parameters whereas the other ones (η_3, η_4, η_5 and η_6) can be generically tagged as "twist" parameters. The following property is useful in understanding the shaping of the $\boldsymbol{\eta}$-spline as affected by its various parameters.

Property 3 *(symmetry) Assume $\eta_1=\eta_2=v\in\mathbb{R}^+$, $\eta_3=-\eta_4=w\in\mathbb{R}$, $\eta_5=\eta_6=z\in\mathbb{R}$ and define $\boldsymbol{\eta}=[v\;v\;w\;-w\;z\;z]^T$. Moreover, consider $\theta_A=\theta_B=\theta\in[0,2\pi)$, $\kappa_A=\kappa_B=0$, $\dot{\kappa}_A=\dot{\kappa}_B=0$ and*

$$
\begin{cases} x_B=x_A+d_1\cos\theta-d_2\sin\theta\\ y_B=y_A+d_1\sin\theta+d_2\cos\theta\end{cases}
$$

where $d_1\in\mathbb{R}^+$ e $d_2\in\mathbb{R}$. Then it follows that

$$
\mathbf{p}(1-u;\boldsymbol{\eta})=\mathbf{p}_A+\mathbf{p}_B-\mathbf{p}(u;\boldsymbol{\eta}) \qquad (24)
$$

$\forall u\in[0,1]$, $\forall v\in\mathbb{R}^+$, $\forall w\in\mathbb{R}$, $\forall z\in\mathbb{R}$.

Proof. By direct substitution into (8)-(23) of all the posed assumptions and after some computations we obtain:

$$
\begin{aligned}
\mathbf{p}(u;\boldsymbol{\eta}) &= \begin{bmatrix}x_A\\ y_A\end{bmatrix}+v\begin{bmatrix}\cos\theta\\ \sin\theta\end{bmatrix}u+\frac{1}{2}w\begin{bmatrix}\cos\theta\\ \sin\theta\end{bmatrix}u^2+\frac{1}{6}z\begin{bmatrix}\cos\theta\\ \sin\theta\end{bmatrix}u^3\\
&+\begin{bmatrix}\cos\theta & -\sin\theta\\ \sin\theta & \cos\theta\end{bmatrix}\begin{bmatrix}35d_1-35v-\frac{45}{2}w-\frac{5}{6}z\\ 35d_2\end{bmatrix}u^4+\\
&+\begin{bmatrix}\cos\theta & -\sin\theta\\ \sin\theta & \cos\theta\end{bmatrix}\begin{bmatrix}-84d_1+84v+17w+\frac{3}{2}z\\ -84d_2\end{bmatrix}u^5+\\
&+\begin{bmatrix}\cos\theta & -\sin\theta\\ \sin\theta & \cos\theta\end{bmatrix}\begin{bmatrix}70d_1-70v-14w-\frac{7}{6}z\\ 70d_2\end{bmatrix}u^6+\\
&+\begin{bmatrix}\cos\theta & -\sin\theta\\ \sin\theta & \cos\theta\end{bmatrix}\begin{bmatrix}-20d_1+20v+4w+\frac{1}{3}z\\ -20d_2\end{bmatrix}u^7
\end{aligned} \qquad (25)
$$

Using the above expression (25) for $\mathbf{p}(u;\boldsymbol{\eta})$ we verify that relation (24) holds $\forall u\in[0,1]$, $\forall v\in\mathbb{R}^+$, $\forall w\in\mathbb{R}$, $\forall z\in\mathbb{R}$. □

The above symmetry property is illustrated in the figures 2, 3, and 4. All these plots describe the so called "lane change"

curve	$\mathbf{p}_A$	$\mathbf{p}_B$	θ_A	θ_B	κ_A	κ_B	$\dot{\kappa}_A$	$\dot{\kappa}_B$	η_1, η_2	$\eta_3, \eta_4, \eta_5, \eta_6$
1	$\begin{bmatrix} 0.3 \\ 0.3 \end{bmatrix}$	$\begin{bmatrix} 1.3 \\ 3.3 \end{bmatrix}$	$\pi/2$	$\pi/2$	0	0	-8	0	3.162	0
2	$\begin{bmatrix} 0.3 \\ 0.3 \end{bmatrix}$	$\begin{bmatrix} 1.3 \\ 3.3 \end{bmatrix}$	$\pi/2$	$\pi/2$	0	0	0	0	3.162	0
3	$\begin{bmatrix} 0.3 \\ 0.3 \end{bmatrix}$	$\begin{bmatrix} 1.3 \\ 3.3 \end{bmatrix}$	$\pi/2$	$\pi/2$	0	0	8	0	3.162	0

Table 1: Path data of figure 5.

curve	$\mathbf{p}_A$	$\mathbf{p}_B$	θ_A	θ_B	κ_A	κ_B	$\dot{\kappa}_A$	$\dot{\kappa}_B$	η_1, η_2	$\eta_3, \eta_4, \eta_5, \eta_6$
1	$\begin{bmatrix} 0 \\ 0 \end{bmatrix}$	$\begin{bmatrix} 4.8764 \\ 0.8186 \end{bmatrix}$	0	0.5	0	0,2	0,04	$-0,36$	4,944	0
2	$\begin{bmatrix} 0 \\ 0 \end{bmatrix}$	$\begin{bmatrix} 4.8764 \\ 0.8186 \end{bmatrix}$	0	0.5	0	0,2	0,04	0,04	4,944	0
3	$\begin{bmatrix} 0 \\ 0 \end{bmatrix}$	$\begin{bmatrix} 4.8764 \\ 0.8186 \end{bmatrix}$	0	0.5	0	0,2	0,04	0,44	4,944	0

Table 2: Path data of figure 6.

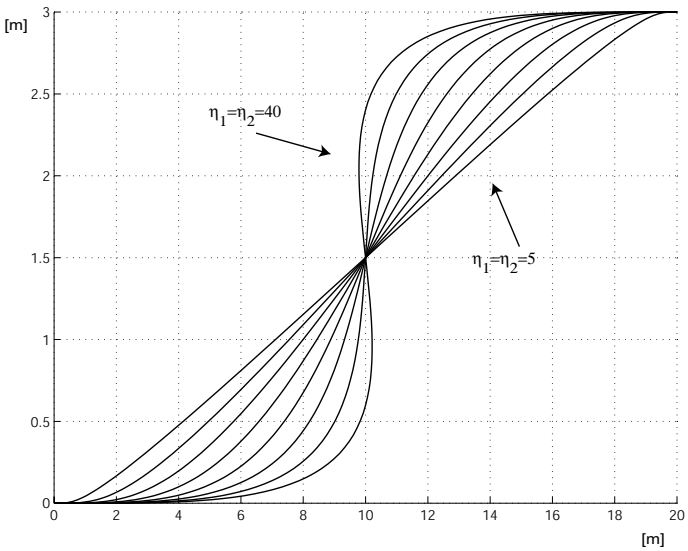

Figure 2: A lane change with $\eta_3 = \eta_4 = \eta_5 = \eta_6 = 0$.

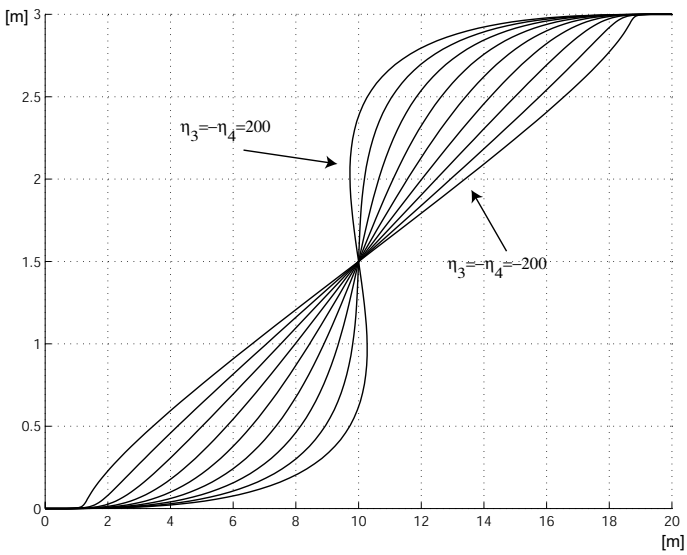

Figure 3: A lane change with $\eta_1 = \eta_2 = 20$ and $\eta_5 = \eta_6 = 0$.

paths with $\mathbf{p}_A = [0\ 0]^T$, $\mathbf{p}_B = [20\ 3]^T$, $\theta_A = \theta_B = 0$, $\kappa_A = \kappa_B = 0$, $\dot{\kappa}_A = \dot{\kappa}_B = 0$, and various choices for the η_i parameters.

As exposed in [5] it is sensible to choose vector $\boldsymbol{\eta}$ by solving a suitable optimization problem. For the G^3-splines the optimal smoothness of the path may be gained by minimizing the absolute value of the variations of $\dot{\kappa}(s)$ along the path, i.e. $\min_{\eta \in \mathcal{H}} \max_{s \in [0, f(1)]} |\ddot{\kappa}(s; \boldsymbol{\eta})|$. This is a difficult minimax problem, however a rough sub-optimal solution is given, in many typical cases of the autonomous robot navigation, by the euristic rule $\eta_1 = \eta_2 = \|\mathbf{p}_A - \mathbf{p}_B\|$ and $\eta_3 = \eta_4 = \eta_5 = \eta_6 = 0$. In figure 5 we have applied this rule to a line change with perturbations on the curvature derivative at the initial path point (see Table 1). These perturbations have a marked effect on the initial shape of the $\boldsymbol{\eta}$-spline. The same rule is also used in figure 6 where the central path is a very good approximation of a clothoid, i.e. $\dot{\kappa}(s) \simeq 0.04\ \forall\, s \in [0, f(1)]$, and the other paths are obtained by perturbing $\dot{\kappa}_B = 0.04 \pm 0.40$ (see all the path data on Table 2).

5 Conclusions

We have presented a closed-form parameterization of seventh-order polynomial splines that permits the planning of composite paths ensuring an overall third-order geometric continuity. This new motion primitive appears especially useful for the smooth iterative steering of autonomous wheeled mobile robots.

Acknowledgements

This work was partially supported by MIUR scientific research funds under the framework of the COFIN projects.

References

[1] Barsky, B. A. and Beatty, J. C.: 1983, Local control of bias and tension in beta-spline, *Computer Graphics* **17**(3), 193–218.

[2] Delingette, H., Hébert, M. and Ikeuchi, K.: 1991, Trajectory generation with curvature constraint based on energy

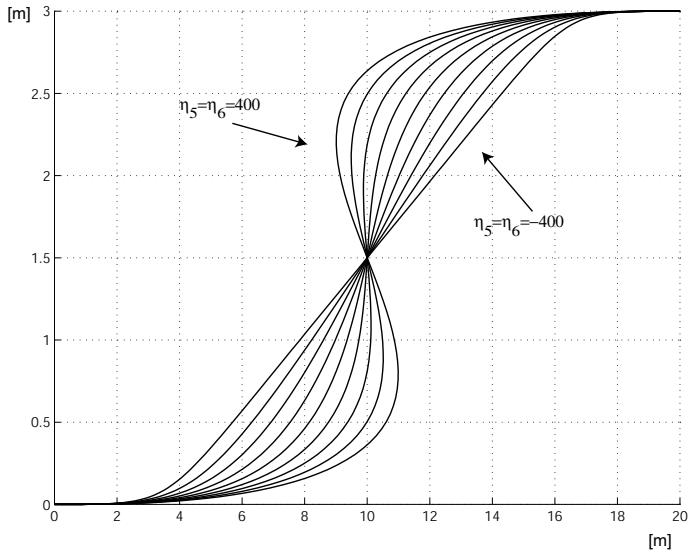

Figure 4: A lane change with $\eta_1 = \eta_2 = 20$ and$|; \eta_3 = -\eta_6 = 100$.

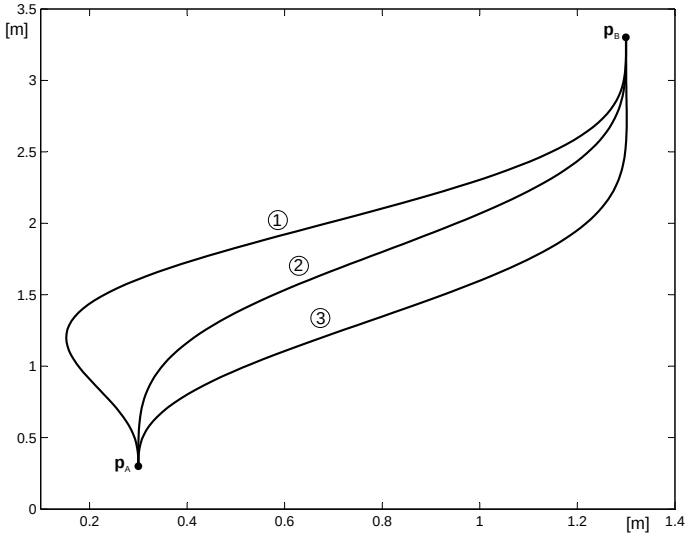

Figure 5: Modifying a line change by perturbing $\dot{\kappa}_A$.

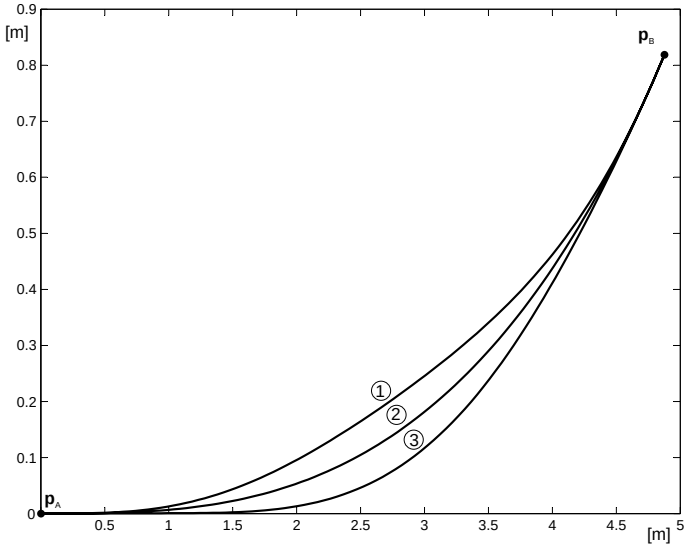

Figure 6: Modifying a clothoid by perturbing $\dot{\kappa}_B$.

minimization., *Proc. of the IEEE-RSJ Int. Conf. on Intelligent Robots and Systems*, Osaka, Japan, pp. 206–211.

[3] Fleury, S., Souères, P., Laumond, J.-P. and Chatila, R.: 1993, Primitives for smoothing paths of mobile robots, *Proceedings of the IEEE Int. Conference on Robotics and Automation*, Atlanta, GA, pp. 832–839.

[4] Fraichard, T. and Ahuactzin, J.-M.: 2001, Smooth path planning for cars, *Proceedings of the 2001 IEEE International Conference on Robotics & Automation*, Seoul, Korea, pp. 3722–3727.

[5] Guarino Lo Bianco, C. and Piazzi, A.: 2000, Optimal trajectory planning with quintic G^2-splines, *Proceedings of the IEEE Intelligent Vehicles Symposium*, Dearborn (MI), USA, pp. 620–625.

[6] Guarino Lo Bianco, C. and Piazzi, A.: 2002, Inversion-based control of wheeled mobile robots, *Proceedings of the IEEE Intelligent Vehicles Symposium*, Versailles, France, pp. 190–195.

[7] Lucibello, P. and Oriolo, G.: 1996, Stabilization via iterative state steering with application to chained-form systems, *Proceedings of the 35th IEEE Conference on Decision and Control*, Vol. 3, Kobe, Japan, pp. 2614–2619.

[8] Nelson, W.: 1989, Continuous steering-function control of robot carts, *IEEE Transactions on Industrial Electronics* **36**(3), 330–337.

[9] Piazzi, A. and Guarino Lo Bianco, C.: 2000, Quintic G^2-splines for trajectory planning of autonomous vehicles, *Proceedings of the IEEE Intelligent Vehicles Symposium*, Dearborn (MI), USA, pp. 198–203.

[10] Piazzi, A., Guarino Lo Bianco, C., Bertozzi, M., Fascioli, A. and Broggi, A.: 2002, Quintic G^2-splines for the iterative steering of vision-based autonomous vehicles, *IEEE Transactions on Intelligent Transportations Systems* **3**(1), 27–36.

[11] Piazzi, A., Romano, M. and Guarino Lo Bianco, C.: 2003, Smooth path planning for wheeled mobile robots using G^3-splines, *Technical Report TSC-02/03*, Dipartimento di Ingegneria dell'Informazione, Università di Parma.

[12] Scheuer, A. and Fraichard, T.: 1996, Planning continuous-curvature paths for car-like robots, *Proceedings of the 1996 IEEE/RSJ International Conference on Intelligent Robots and Systems*, Osaka, Japan, pp. 1304–1311.